

**METHODS OF DIGITAL SIGNAL ANALYSIS APPLIED TO THE STUDY
OF DYNAMIC SYSTEMS IN HELICOPTERS**

by

**J.P. COSTON – Test Engineer
Aerospatiale Helicopter Division
Marignane – France**

**FIFTH EUROPEAN ROTORCRAFT AND POWERED LIFT AIRCRAFT FORUM
SEPTEMBER 4 – 7 TH 1979 - AMSTERDAM, THE NETHERLANDS**

1 - SUMMARY

The first part of this paper concerns the synchronous method of analysis. The traditional clock frequency governing analog-to-digital converters is replaced by a pulse train coming directly from the rotating unit which has a built-in coder.

This method has three basic advantages :

- uncertainties of analysis are minimized
- the processing rate is accelerated by the reduction in the number of points calculated
- the results obtained have a direct, physical meaning.

The discussion is followed by some examples taken from specific analyses. (Tests on rotating blades, a study of gear meshing noise).

The second part of the paper describes an approach to using the coherence function and the power spectrum to determine the principal modes of blades rotating on test rigs. The problems experienced, mainly due to the low response level of blades without any forward speed, should not lead us to underestimate the potential of this approach.

2 - SYNCHRONOUS ANALYSIS

2.1 - BACKGROUND

Any digital acquisition of signals always occurs over a limited time interval. The characteristics of the Fourier series, which are generally calculated after signal acquisition will be directly related to the parameters for defining that interval. (see Fig. 1).

The process of digital acquisition, to describe it schematically, always amounts to multiplying the signal to be processed $x(t)$, whose duration is theoretically infinite, by a "window" function $W(t)$ known as the weighing function, which is generally a unit element of finite duration T . After analog-to-digital conversion and quantification, this results in a discrete signal $x(k \Delta t)$ with N samples. Synchronous analysis essentially means giving a physical meaning to the 'window' function $W(t)$.

This function is defined by two basic parameters :

- the initial instant t_0
- the duration T

Synchronous analysis thus consists in giving a physical meaning to these two parameters.

Most signals processed in helicopter systems, subject to verification of stationarity criteria which will not be dealt with here, result from a cyclic type of process with a complex periodic law (revolving systems in general).

Assume a revolving mobile related to a system of rotating axes (M) of origin (O), a point on the axis of rotation for example.

Let us assume also an absolute reference (F) of the same origin (O).

- The instant t_0 corresponds to the coincidence of the two axis systems (M) and (F). This is called the instant of synchronization.

- The duration T corresponds to the period of rotation T_0 of system (M), or to a multiple of it.

For the sake of simplicity, let us take the case where $T = T_0$.

Thus, the conversion of the continuous multi-level signal $x(t)$ in the time interval T_0 into a discrete signal $x(k\Delta t)$ with N samples, will have to satisfy this criterion :

$$(1) \quad \frac{T_0}{N} = \Delta t \quad \text{sub-multiple of } T_0$$

The algorithm of the fast Fourier transform requires :

$$N = 2^{k_1} \quad k_1 \text{ integer } > 0$$

The value of Δt , called the sampling period, must therefore depend on, and be proportional to, that of T_0 . (Δt is also called the clock period).

Thus where :

$$f_0 = \frac{1}{T_0} \quad \text{system (M) frequency of rotation}$$

$$f_e = \frac{1}{\Delta t} \quad \text{sampling frequency}$$

$$(1) \text{ is written } f_e = N f_0 = 2^{k_1} f_0$$

The sampling frequency is thus a multiple of the fundamental frequency of the system being analyzed, using a power factor of 2.

Shannon's theory of sampling gives us a maximum analyzed frequency f_M , such that :

$$f_M = \frac{f_e}{K}$$

K in general, from the form $K = 2^{(k_2 + 1)}$

$$k_2 \text{ integer } \geq 0$$

$$\text{therefore } f_0 = \frac{f_M}{2^{(k_1 - k_2 - 1)}}$$

in the extreme case authorized, $k_2 = 0$

$$\text{i.e. } f_0 = \frac{f_M}{2^{(k_1 - 1)}}$$

Thus, whatever the variation of f_{ox} over a period of time, the maximum frequency analyzed will always verify :

$$\frac{f_M}{f_0} = 2(k_1 - 1) \quad \text{a frequency value which}$$

can be calculated with the maximum of precision.

In addition to the precision, it should be noted that there are $2(k_1 - 1)$ calculation values for frequency, each representing an order of harmonics between 1 and $[2(k_1 - 1) - 1]$.

In the case of the common value $k_1 = 6$, the analysis can thus be extended to the 31st order.

A value of $k_1 = 4$, where analysis is possible to the 7th order of harmonics, is far more realistic. The number of samples to be taken is reduced (16) and calculation time can be shortened appreciably.

This method thus has the combined advantages of precision and speed.

Lastly, once the instant t_0 has been defined, the two components, real and imaginary, for each of the terms of the series calculated, also take on a physical meaning. It is thus possible, e.g. for average calculations, to add then directly term to term, according to the samples (which greatly increases the speed of processing programmes) without relinquishing the notion of phase.

2.2 - EXAMPLES OF USES

2.2.1 - Determining the specific modes of rotor blades rotating on a rig

Main and tail rotor blades are tested on a rig exactly reproducing the complete power transmission system. There are two basic differences from normal flight conditions :

- ground effect
- absence of forward speed.

Two types of tests are carried out ; they are illustrated by the following frequency diagrams :

2.2.1.1 - Determination of mode crossing points. Influence of modes on the rotor harmonics responses, at nominal speed.

See Fig. 2 :

The rotors are fitted with digital coders delivering 2^{k_1} pulses per revolution.

An azimuthal coder makes it possible to cut off the signal acquisition (value t_0) for a given rotor azimuth, and in relation to the bench axes.

The signals sampled are generally sent by a series of gauge stations measuring flapping or drag bending moments, according to the mode to be analyzed, these being fitted to the blade span.

It should be noted that, during these tests, the blades may have to be made to vibrate artificially, for example by using the pitch control, because of the low response that sometimes occurs. The cause is often aerodynamic damping specific to the flapping modes especially.

In such cases, hydraulic vibration exciters are fitted in place of the servo-controls. A processing unit generates a complex sine control signal, made up as desired of 1Ω , 2Ω , 3Ω , 4Ω to the 10^{th} order, which controls the vibration exciters. This signal comes from a reversible counter system in the processing unit and is guided by the sampling pulse train from the coder fitted on the rotor head.

Vibration frequency variation is thus directly achieved by means of the rotor speed control.

See Fig. 3.

The diagram in Fig. 4 sums up the general principle.

See Fig. 4.

2.2.1.2 - Frequency position of modes

See Fig. 5.

The excitation method is exactly as in the previous description.

As a general rule, rotor speed and pitch remain stabilized during frequency scanning.

The coder previously fitted to the rotor head is replaced by a pulse generator. The pulse train provides signal sampling and the control of the hydraulic exciters via the processing unit mentioned above.

For this test, the frequency scanning is done with constant collective pitch excitation of about $\pm 1^\circ$. The stress response of a gauge fitted to the blade is measured, and also the phase relative to the pitch applied.

To demonstrate dissymmetric modes, it may be necessary to excite the blades while applying cyclic pitch, whether in the direction of rotation or in the opposite direction. The analyzer unit will in that case allow for shifts in rotor Ω .

By further processes with several gauge stations, and by knowledge of spanwise curvature, it is possible to identify the mode being examined.

This vibration is shown in Fig. 6.

Usually, several tests of this type are done at different speeds, so that the frequency diagram can be completed.

A few examples

- * A study of the effect of a tail rotor drag mode on the 3Ω level.

At nominal rotor speed, the natural frequency of the mode increases with pitch until it crosses 3Ω .

See Fig. 7 for a study using natural vibration.

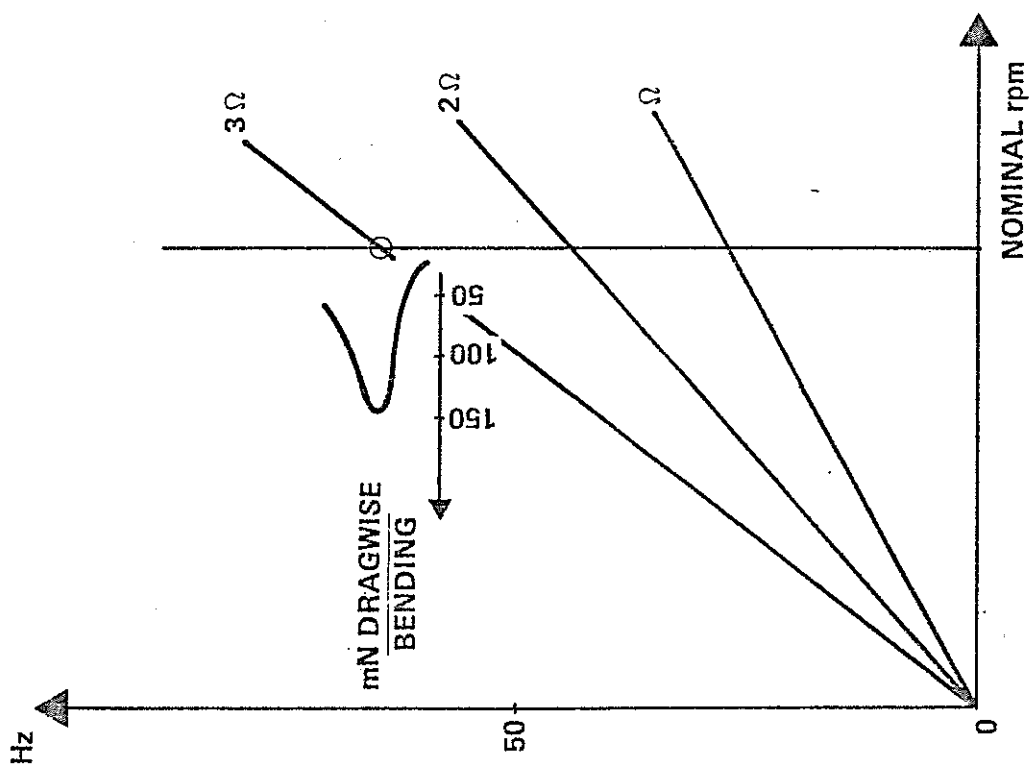
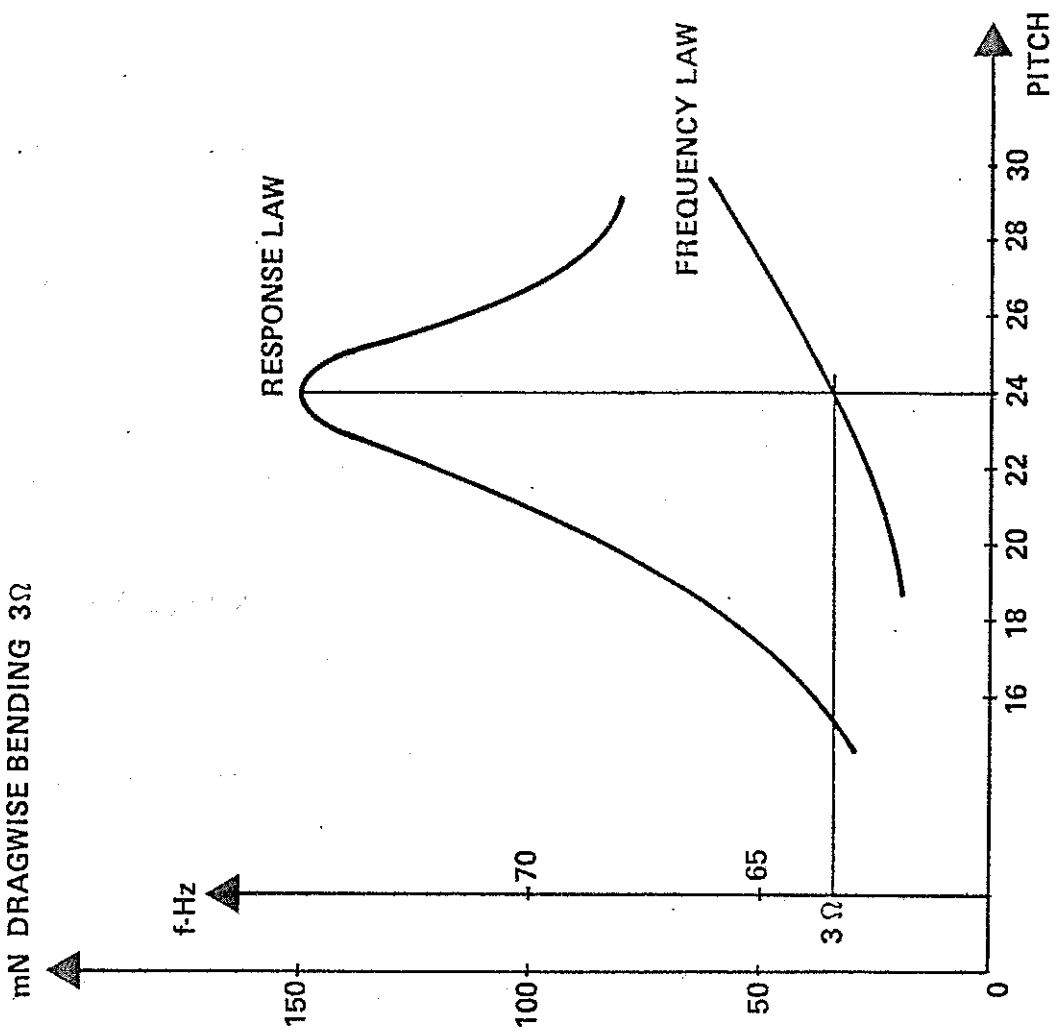


Fig. 7 — Study of the effect of a tail rotor drag mode on the level of 3rd harmonic.

* Main rotor blade flap and drag mode responses, with collective pitch applied, at different r.p.m. values. See Fig. 8.

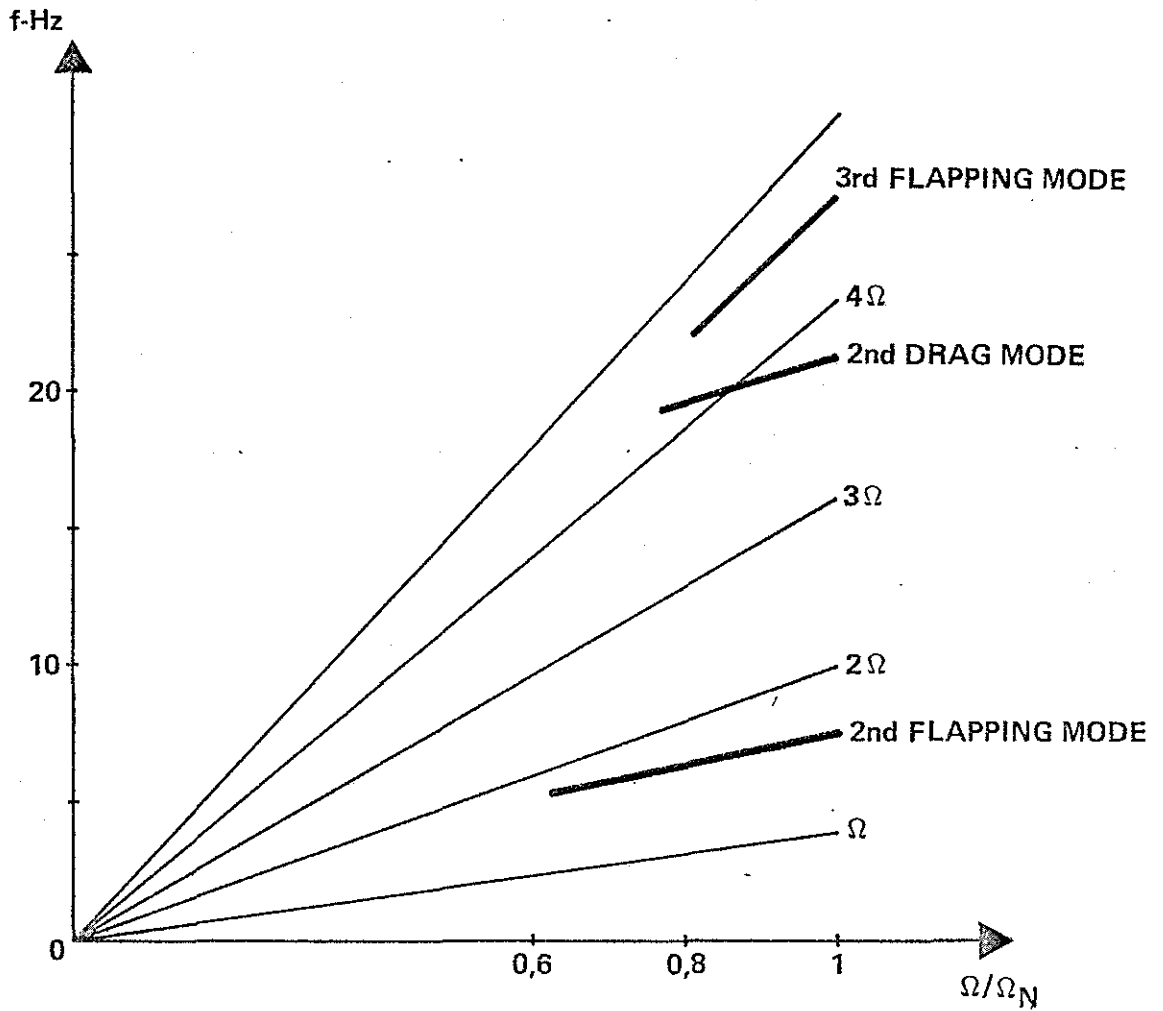


Fig. 8 — Main rotor blade flap and drag mode responses, with collective pitch applied, at different r.p.m. values.

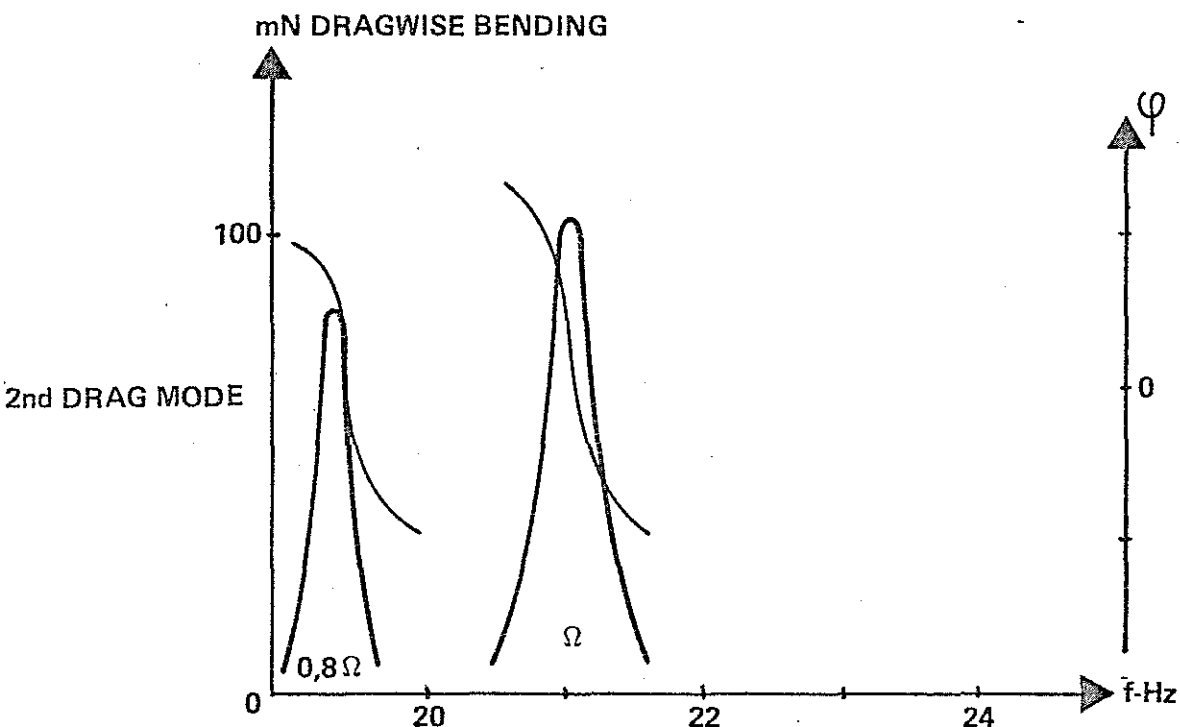
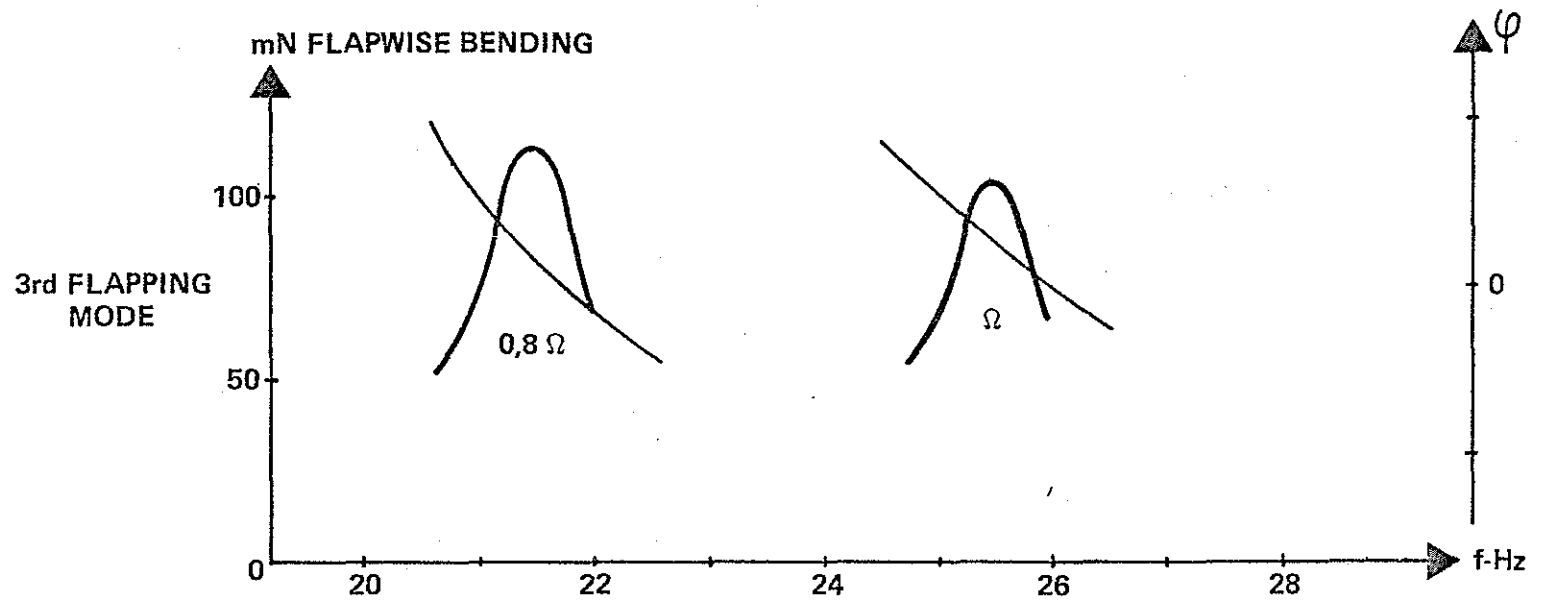
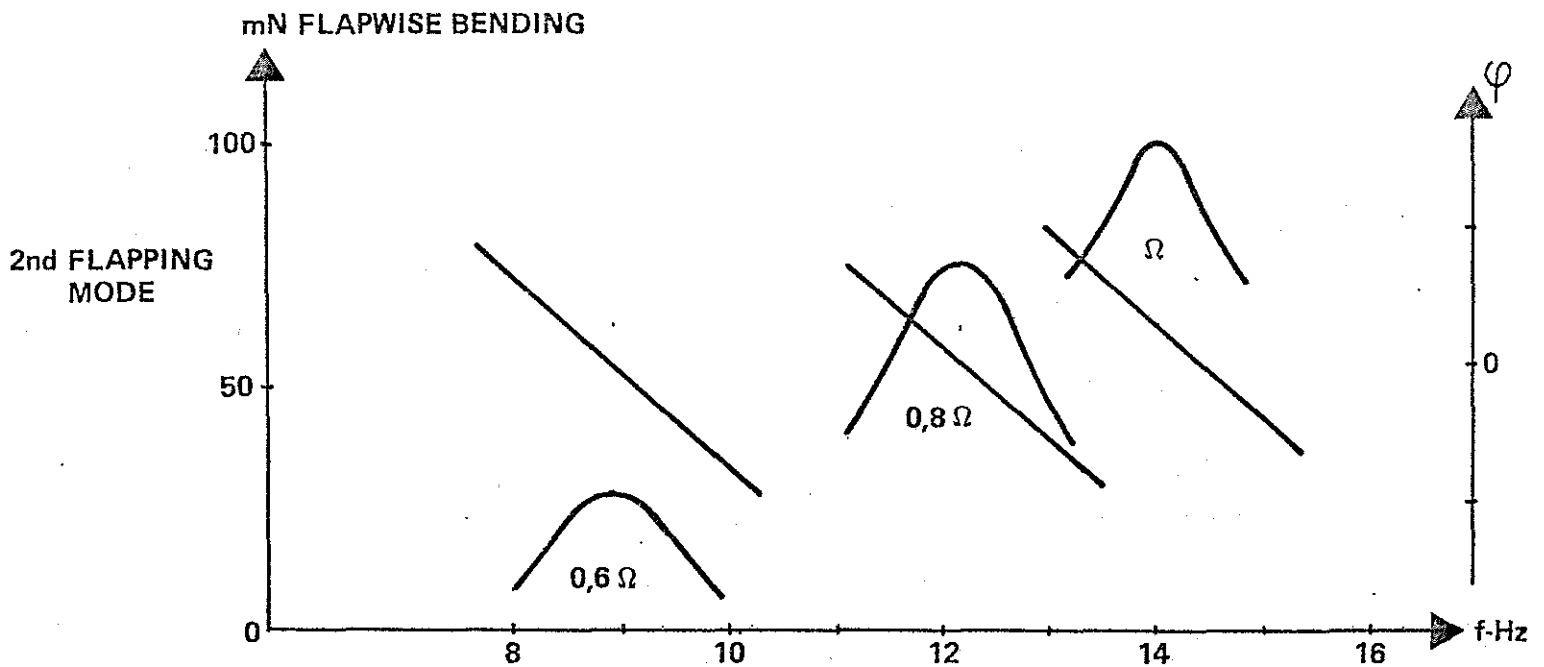


Fig. 8 — Main rotor blade flap and drag mode responses, with collective pitch applied, at different r.p.m. values.

2.2.2 - Study of gearbox meshing noise

The application of synchronous analysis to this type of study has two objectives :

- to eliminate interference noise
- to improve the method of analysis by using synchronous detection.

The method remains essentially the same as described above.

To a gearbox mechanical output is attached a coder which, again, starts signal acquisition and sampling frequency. In the case of an MGB, the output used will generally be the tail rotor power take-off flange, whose r.p.m. are usually mid-way between the highest, at the gearbox input, and the lowest which are to be found at its output.

This type of analysis takes advantage of the physical reality of both components of each term in the series calculated.

Thus, taking a complex signal from a microphone located in a noise field near an operating gearbox, it is possible, using synchronous analysis applied to the average value of the signal received, to isolate the signal by progressive cancelling out of the unwanted components whose frequencies are not multiple of the acquisition.

In contrast to conventional spectrum analysis, this method enables us to retain the notion of phase for each of the spectrum lines observed (fundamental and harmonics) and to work farther to the profile of the acoustic pressure waves given out by the gear mesh observed. Thus, in addition to the noise level in decibels, the gear mesh is identified by the phases of its various components.

There is an immediate practical problem because the inaccessibility of some revolving parts (spiral bevel gear shaft, for example) makes it impossible to install the coders, or their working environment (t⁰, oil) could lead to their rapid deterioration.

Therefore, from pulses delivered by the power take-off flange, coder digital operators such as frequency multipliers and dividers, allow supplying the 2^k pulses per revolution, with synchronization signal start, of any gearbox moving component by merely applying the relevant gear ratios.

To give a general idea, the main noise emissions of a PUMA type main gearbox can be processed with twenty operators of this type.

As an example, we can mention the analysis parameters concerning the study of the spiral bevel gear and epicyclic reduction stage meshing noise of the DAUPHIN type main gearbox. Refer to Fig. 9.

A coder with 2^{10} pulses per revolution is fitted to the power take-off flange.

The sampling pulse frequency is 67 KHz and that of synchronization signal start is 66 Hz.

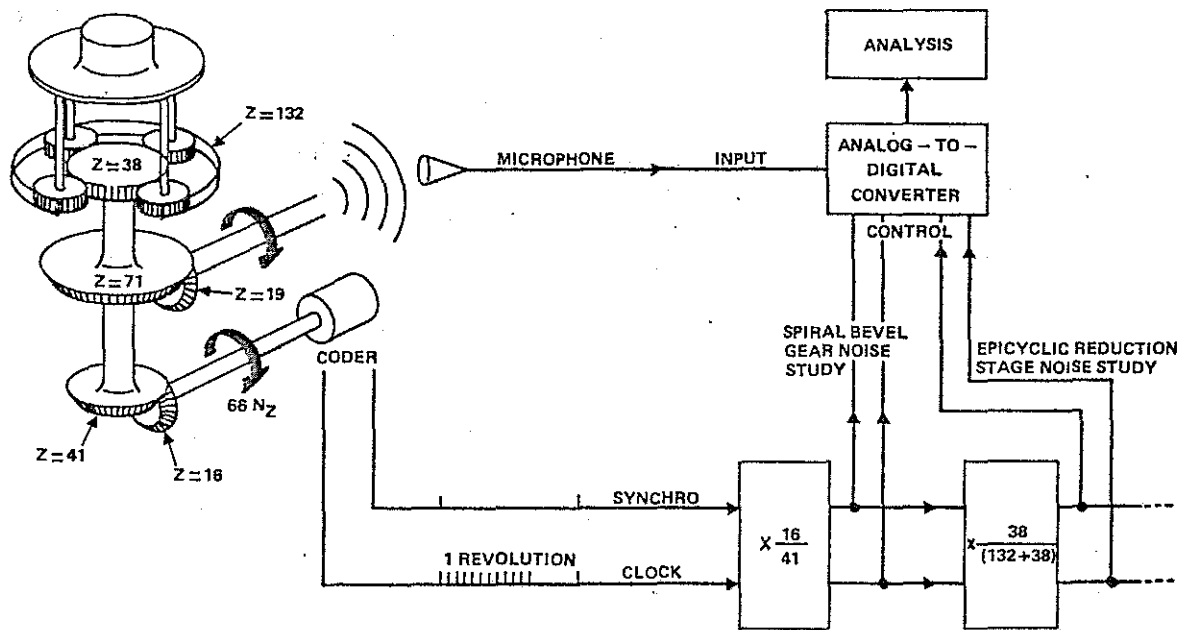


Fig. 9 — Meshing noise study —
 DAUPHIN spiral bevel gear and epicyclic reduction stage
 Functional diagram.

The application of a $\frac{16}{41}$ gear ratio to the pulse train results in 2^{10} pulses per revolution of the spiral bevel ring gear. Then, sampling frequency is 26 kHz.

For a same position of the ring gear, the acquisitions can be initiated by applying the same process to the azimuth signal start.

According to the same principle, the epicyclic reduction stage meshing noise can be studied through a weighting factor multiplied by coefficient $\frac{16}{41} \times \frac{38}{(132+38)}$ and so step by step.

In addition to the immediate advantage drawn from synchronous analysis, two long-term objectives are aimed at :

The first objective is to achieve a meshing frequency simulator from the actual in-flight measured speed, from a group of operators reproducing the gear ratios and from a distortion generator ; such a simulator allows studying the relative effect of each spectrum component in a listening room.

The second objective is to allow for a direct appreciation of the tooth pattern quality of a meshing system in operation through the systematic measurement of acoustic wave shapes largely using the phase parameter.

3 - COHERENCE FUNCTION APPLIED TO THE DETERMINATION OF NATURAL MODES OF ROTATING BLADES

The principle (previously mentioned) of analyzing, the natural modes of rotating blades, presents the drawback of fitting the rotor with external equipment with items such as coders or pulse generators.

In addition to the duration specific to the equipment, the very principle, for safety or lead time reasons, delays its utilization for flight tests.

In view of the above, we were led to consider an analysis method that can suit these various constraints without altering the quality of results.

The only way to provide accuracy without using auxiliary means, such as those previously mentioned, led us naturally to the crossed signal analysis. The phase coherence degree that may exist between two signals from gauge bridges fitted to a rotor blade vibrating to a natural mode was more precisely measured.

3.1 - BACKGROUND

Assuming a linear system with an input signal $x(t)$ whose Fourier transform is $X(f)$ and an output signal $y(t)$ whose Fourier transform is $Y(f)$, the basic function enabling this system to be identified is said the frequency response function (or transfer function) :

$$H(f) = \frac{Y(f)}{X(f)} \quad (1)$$

In practice, since the signals are not quite steady in time, such a constraint requires an estimator of $Y(f)$ and $X(f)$ to be obtained through the use of the average operator.

But, the average of a Fourier transform is significant only if the acquisition instant is physically defined.

The difficulty is got over as follows :

as $X(f)$ is a complex number, its conjugate $X^*(f)$ can therefore be calculated.

Then, equation (1) can be expressed as :

$$H(f) = \frac{Y(f) X^*(f)}{X(f) X^*(f)}$$

The numerator is called cross power spectrum :

$$G_{yx}(f) = Y(f) X^*(f)$$

This is a complex number whose modulus is equal to the product of moduli of $Y(f)$ and $X(f)$ and whose phase is equal to the difference of phases.

It can be noticed all at once that the phase related to the acquisition instant will naturally disappear just by subtraction. Then, $G_{yx}(f)$ can be averaged independently of the acquisition instant :

$$\text{Assuming } \overline{G_{yx}}(f) = \frac{1}{n} \sum_{i=1}^n [G_{yx}(f)]_i$$

The denominator is called input auto power spectrum :

$$G_{xx}(f) = X(f) X^*(f)$$

This is a real number, equal to the square of modulus of $X(f)$.

The following shall be obtain :

$$\overline{G_{xx}}(f) = \frac{1}{n} \sum_{i=1}^n [G_{xx}(f)]_i$$

$$\text{then } H(f) = \frac{\overline{G_{yx}}(f)}{\overline{G_{xx}}(f)} \quad (2)$$

If both equalities (1) and (2) are squared, the following equation is obtained :

$$\overline{G_{xx}}(f) \cdot \overline{G_{yy}}(f) = \left| \overline{G_{yx}}(f) \right|^2$$

Without deeply analyzing this equality, it should however be noted that in practice, it is seldom verified.

Why ?

Whereas in the first term, both factors really correspond to the input and output auto power spectra respectively, on the other hand, the second term should be interpreted with much more care. In fact, due to the average operator, for each frequency, the second term calls out the input/output phase stability depending on the various samplings obtained.

In fact, under certain conditions, what appears at the output may not appear at the input. For example, that is the case of an input parasitic source inducing an output line noise. In that case, average $\overline{G_{xy}}(f)$ will be affected, then $\left| \overline{G_{yx}}(f) \right|^2$ and the previous equality will be the less verified. Thus, the phase coherence degree that may exist between a system input and output can be qualified.

$$\text{Function } \gamma^2 = \frac{|G_{yx}(f)|^2}{G_{xx}(f) G_{yy}(f)}$$

is said "coherence function", that is a positive real function between 0 and 1.

This method for determining the rotating blade modes under natural excitation (each blade is fitted with n flapping and drag bending gauge stations) therefore consists in supposing an equivalent system, one gauge station of which, selected beforehand, in the vicinity of the blade shank, is the input and whose $n-1$ other gauge stations are the outputs.

For a given configuration, the $(n-1)$ coherence functions are therefore first calculated and their results validate the subsequent calculation of the transfer functions, for values close to 1.

Thus are obtained the mode natural frequency and the blade curvature mode shape with respect to the normalization point represented by the system input.

3.2 - APPLICATION EXAMPLES

3.2.1 - Tests on rotating bench without forward speed. Main rotor blades

The test rig is that previously described.

The lessons drawn from the tests are as follows :

On main rotor blades, from 0 to 50 Hz, the sharp coherence zones are clearly localized ; they are of two types :

- rotor harmonics range
- mode response frequencies.

The difference lies in that the transfer function phase in the case of a natural mode response has a value close to $k\pi$; this is not the case for those concerning the harmonics.

The drag modes, especially the second one, offer a very high coherence between 0.9 and 1.

The flapping modes offer lower coherence values near 0.7 to 0.9.

It should be noted that during the test, the sharp coherence zones immediately show the frequency ranges in which dynamic problems will rise.

a) Drag mode measurement — Nominal speed

See Fig. 10.

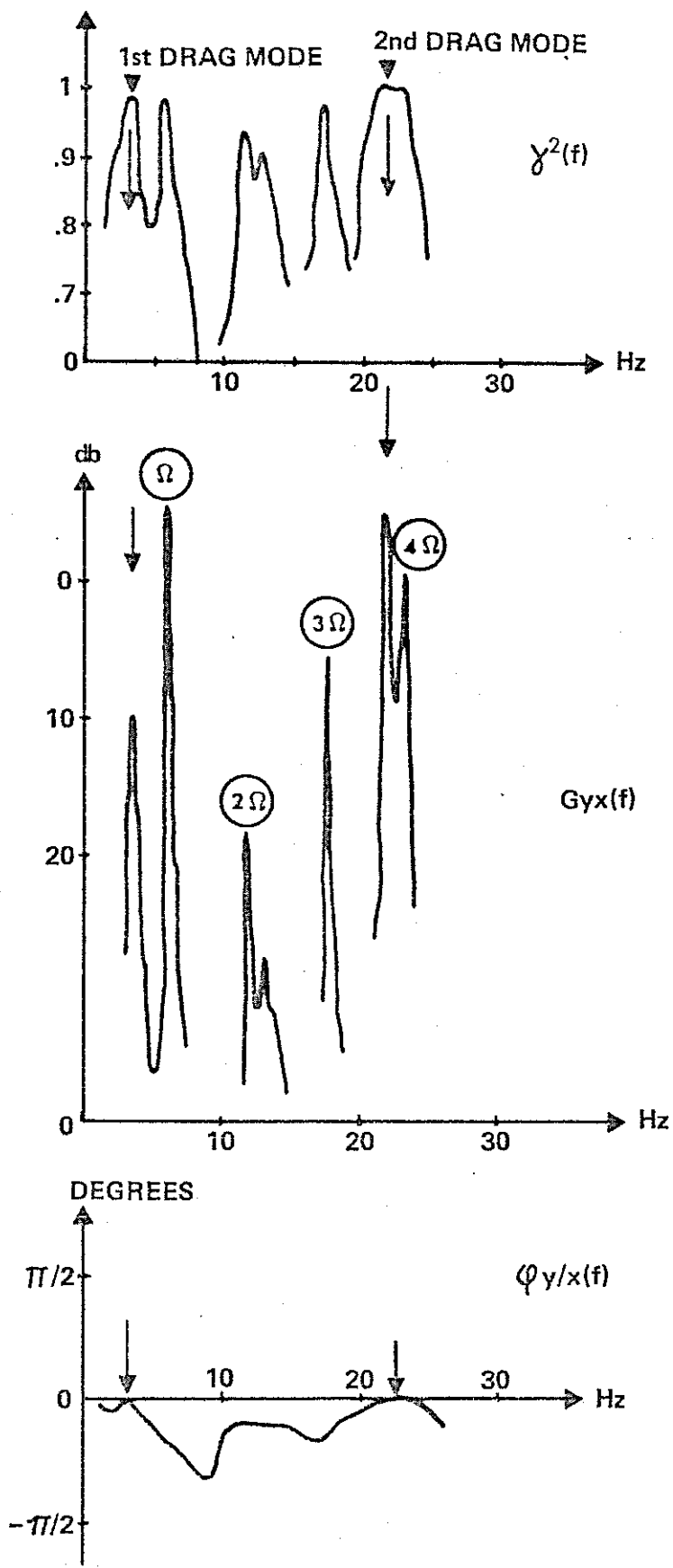


Fig. 10 – Measuring main rotor blade drag modes using the coherence method.

One should note that, in drag, the second flapping mode response (see continuation) occurs close to the 2Ω .

b) Flapping mode measurement

See Fig. 11.

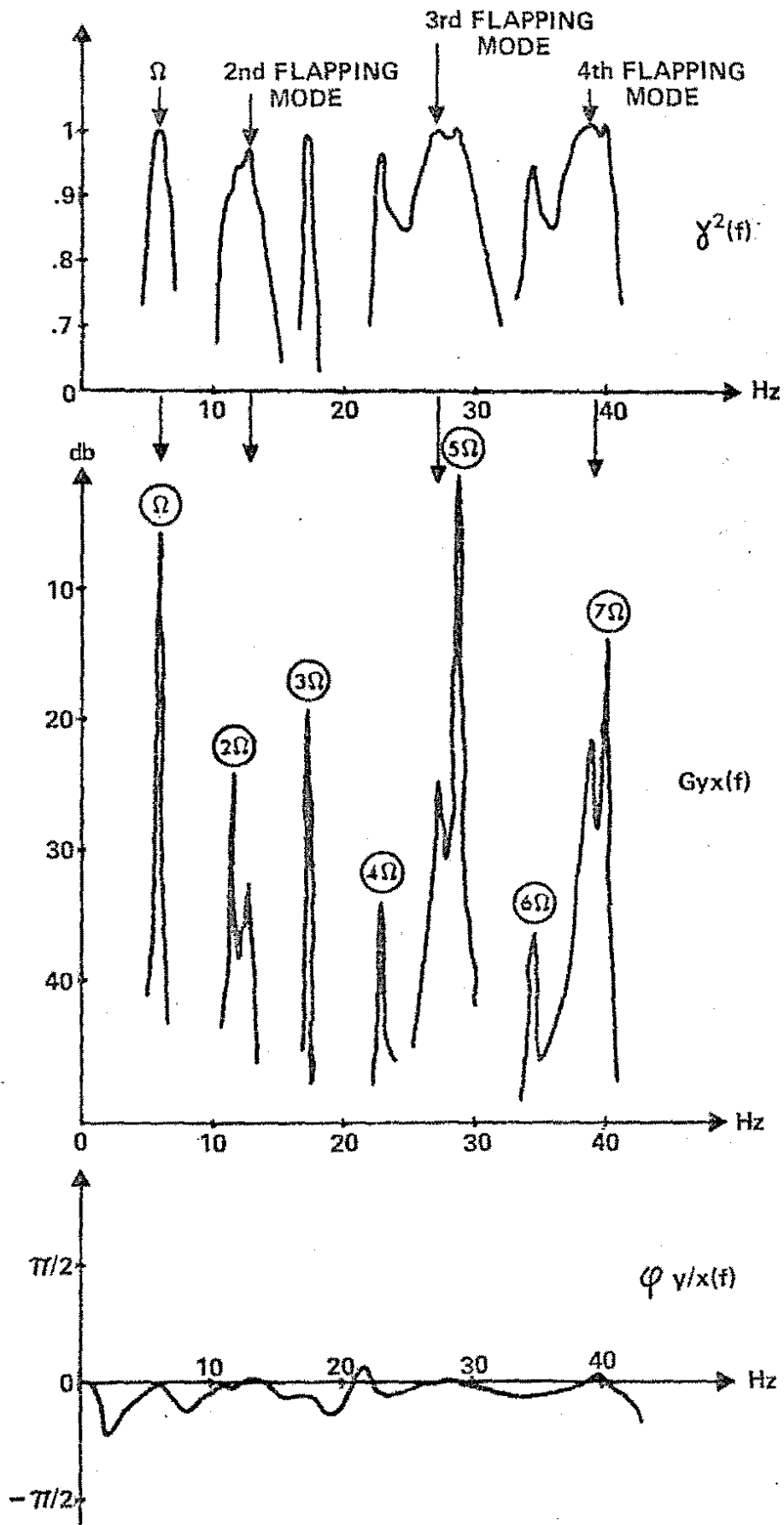


Fig. 11 — Measuring main rotor blade flapping modes using the coherence method.

It should be noted that, as regards the coherence function, the mode levels are nearly the same as those of the harmonics whereas they are far lower for the cross spectrum.

3.2.2 - Tests on aircraft in forward flight. (80 knots)

Considering the constraints associated with the flight and mainly with signal recording, only the rotor blade drag stations were analyzed with a view to identifying the second drag mode. The main rotor blades used were those previously rig tested.

Compared with those latter results, the in-flight measured coherence function shows more important levels (close to 1) on all analyzed harmonics. On the contrary, the response of the second drag mode appears lower. See Fig. 12.

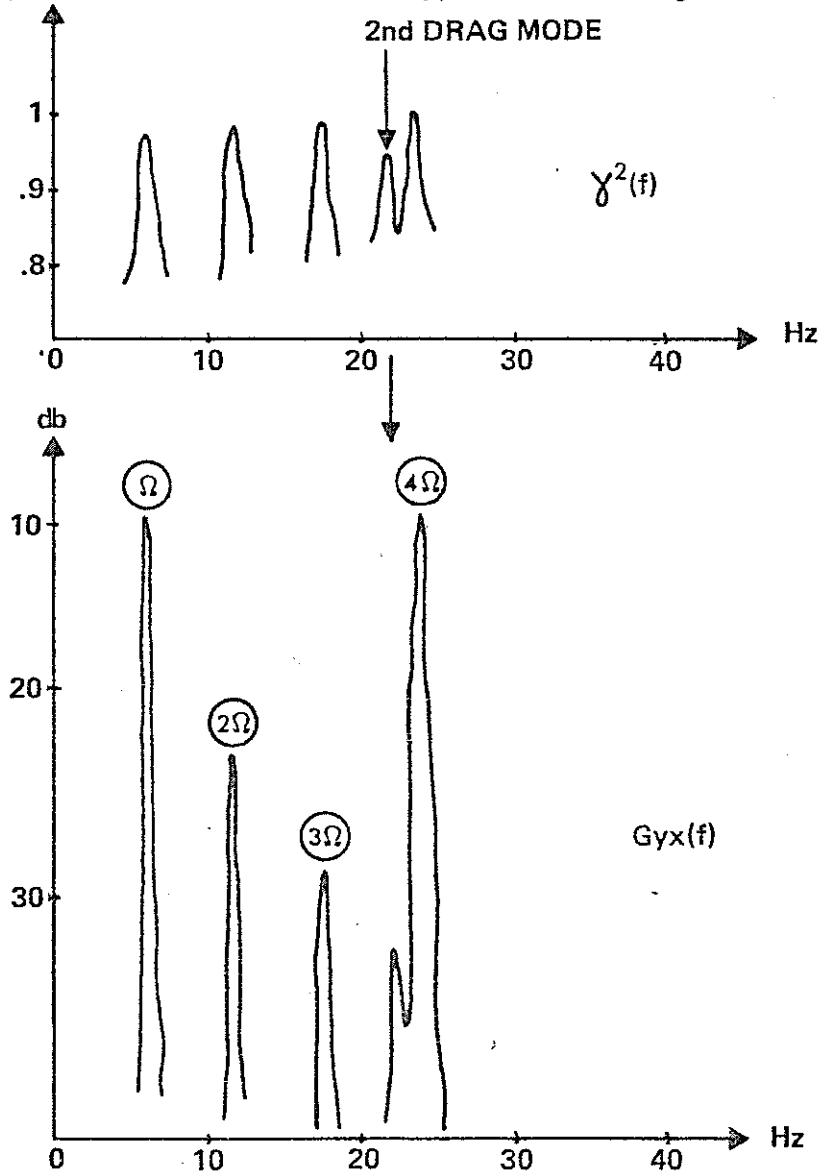


Fig. 12 — Measuring main rotor blade second drag mode — Aircraft in flight.

The result is a confirmation of that obtained on the rig. 2nd drag mode : 3.6 Ω .

3.2.3 - Analyzing a ground resonance phenomenon

A ground resonance phenomenon was experienced during an engine speed rise on ground run.

The fine analysis of rotor blade drag station signals within the 2 to 4 Hz range, leads to results thoroughly summarizing the method principle.

The coherence function is saturated at value 1 from 2.4 to 2.7 Hz ; all the other points are not greater than 0.5.

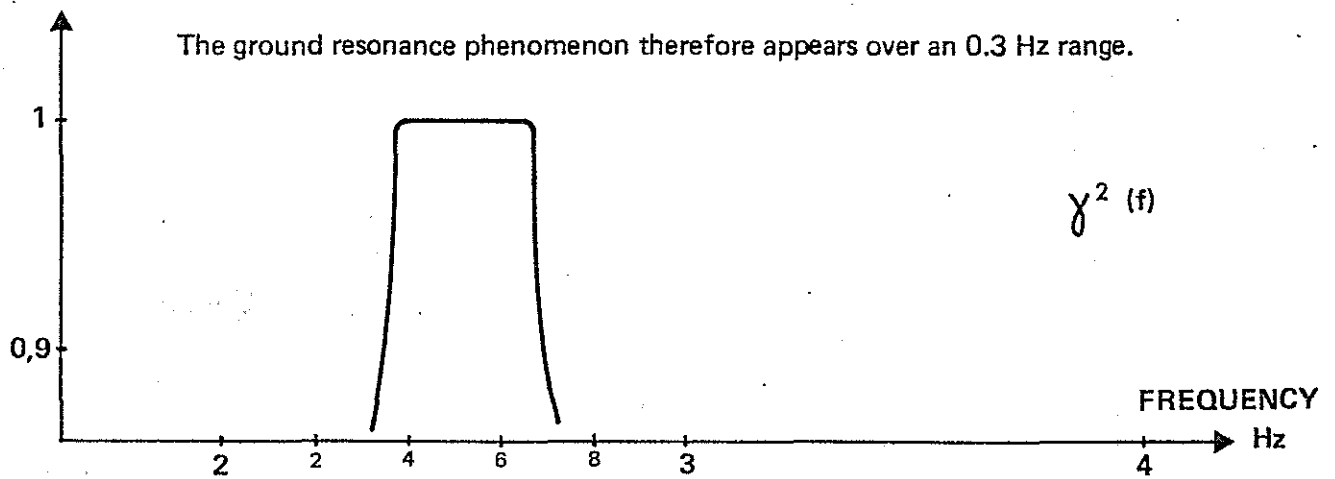


Fig. 13 — Coherence function plotted for a case of ground resonance.

Within this band, the cross spectrum value increases by 40 db approximately with respect to the measurement background noise.

Maximum is obtained at 2.56 Hz.

See Fig. 14.

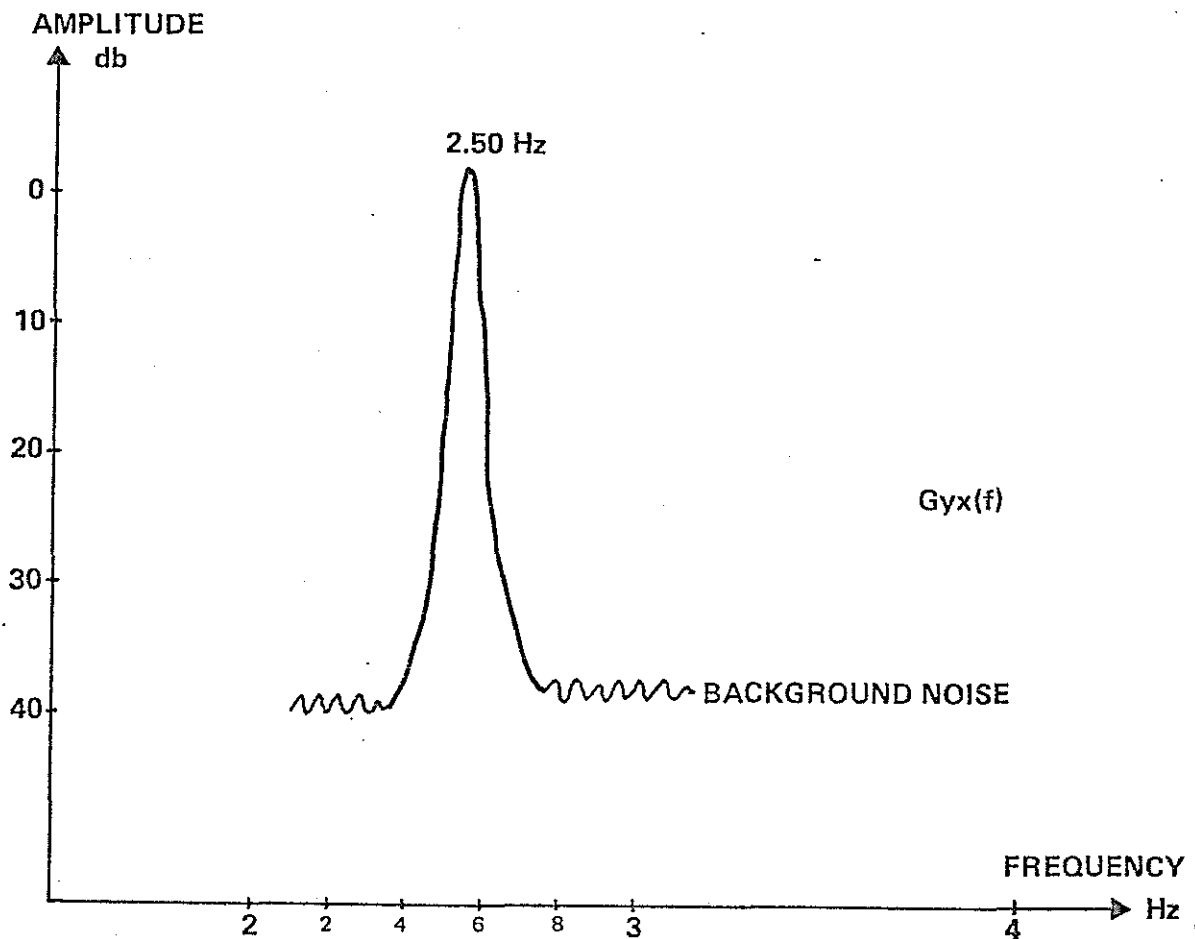


Fig. 14 — Cross-spectrum value on ground resonance.

The phase criterion is strictly established at 0° within the relevant band, the other points should be considered as erroneous due to low dynamic.

See Fig. 15.

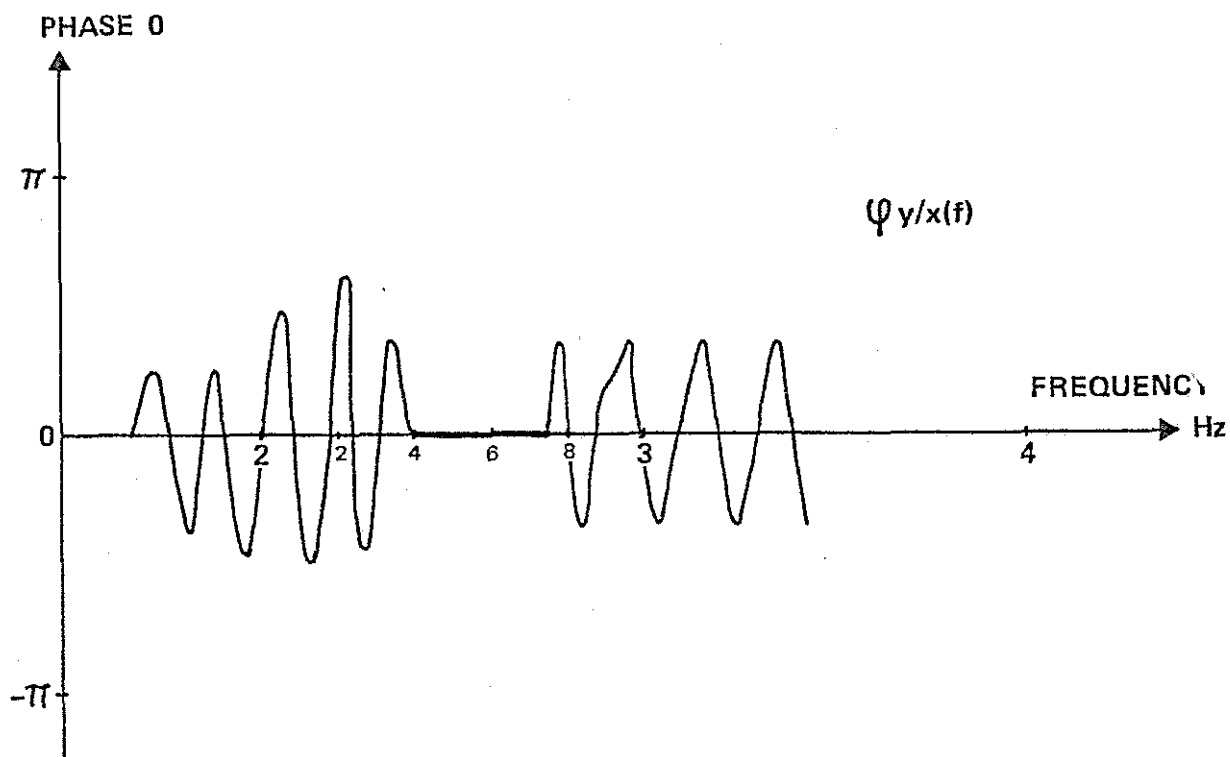


Fig. 15 — Value of phase recorded between two drag stations on ground resonance phenomenon.

An important task is however still to be done on the matter which mainly concerns :

- crossed analysis of flapping/drag responses for coupling survey
- improvement in accuracy of coherence function calculation by using the analysis digital technique in narrow band.

4 - CONCLUSION

As a matter of fact, these methods meet the same requirement as others that could not be detailed here :

– To improve our experimental investigation implement by applying all the solutions offered by the signal analysis technique.

The effort made for reaching a better adaptation of the means to the needs yields physical data which allow expecting a higher comprehension of the phenomenon studied, a more reliable experimental setting together with an adequate cost reduction.

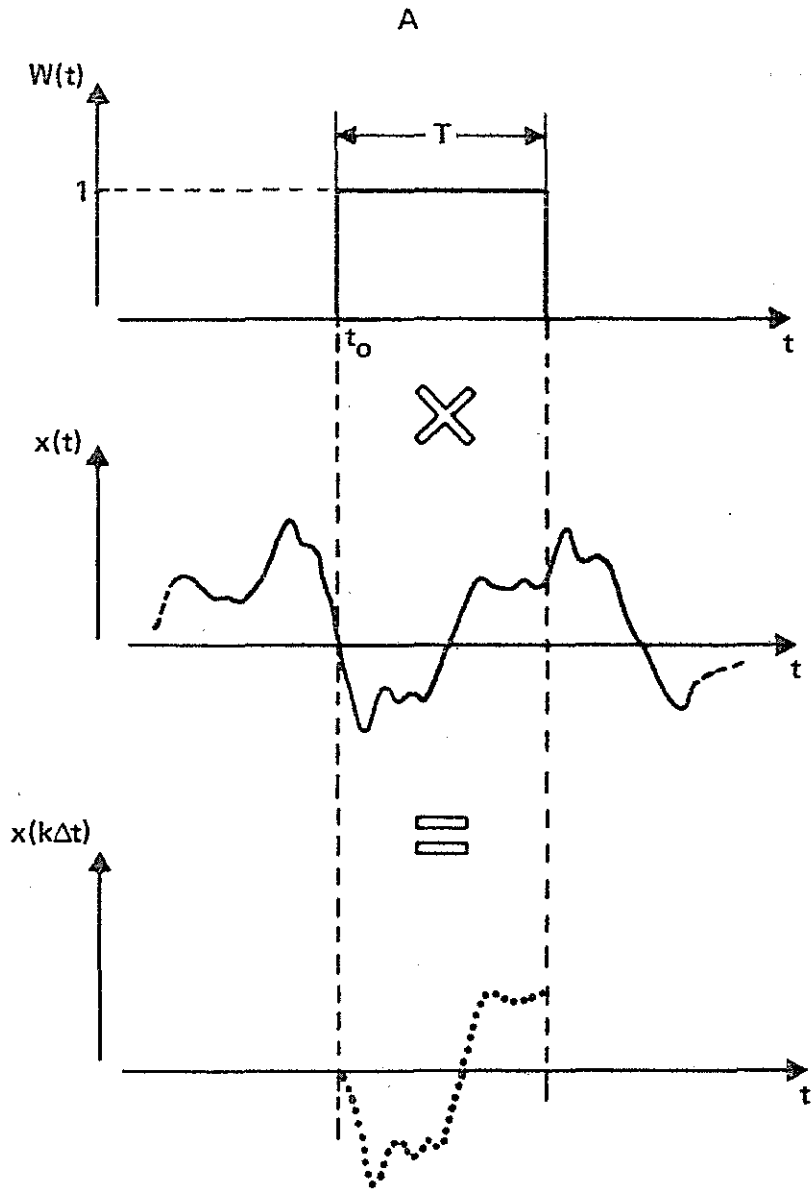


Fig. 1 — Digital acquisition process of an $x(t)$ signal

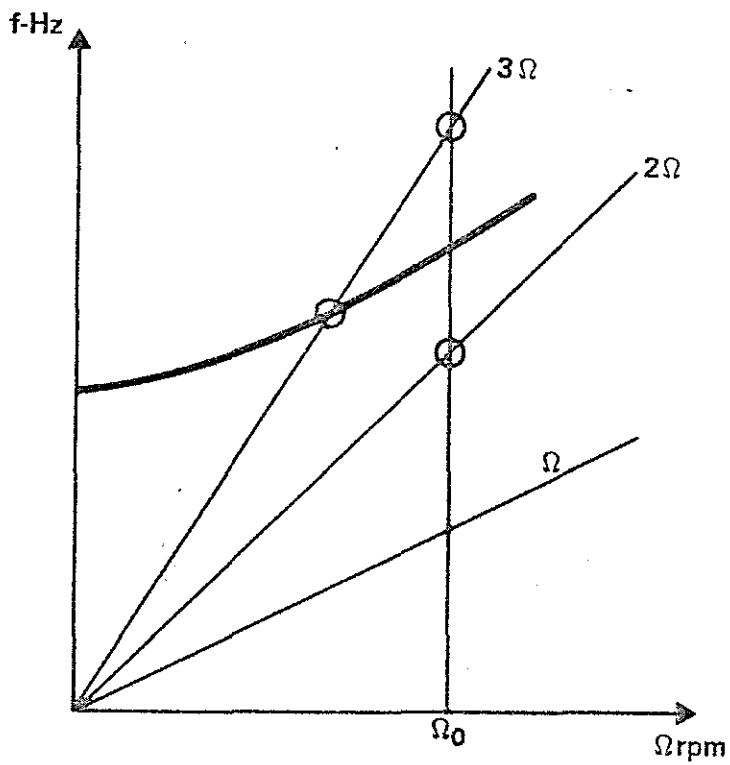


Fig. 2 — Rotor blade mode — Crossing and effect on the rotor harmonics at nominal r.p.m.

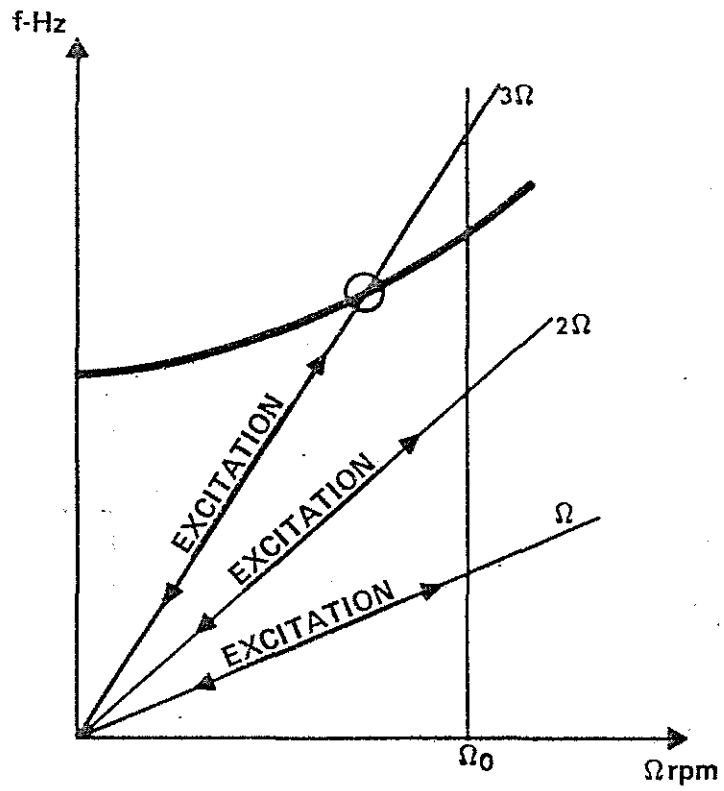


Fig. 3 – Rotor blade mode – r.p.m-slaved excitation principle

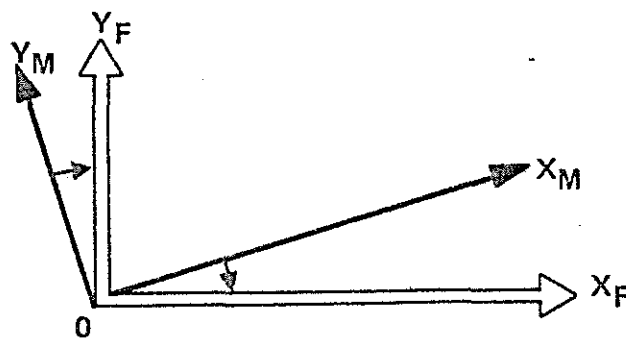
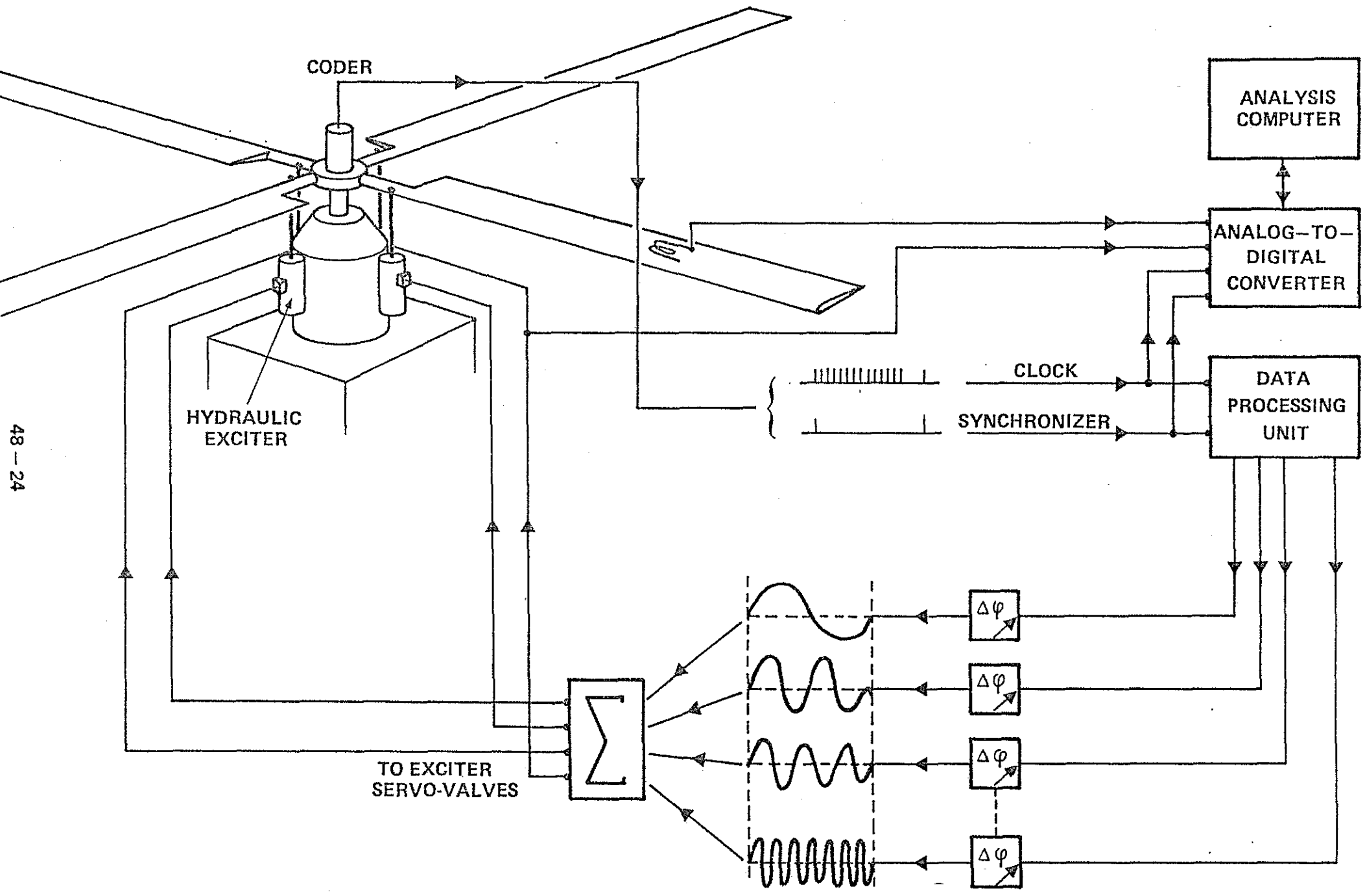


Fig. 4 – Rotor blade mode – General principle of the r.p.m-slaved excitation



48-24

Fig. 4 - Rotor blade mode - General principle of the r.p.m.-slaved excitation

D

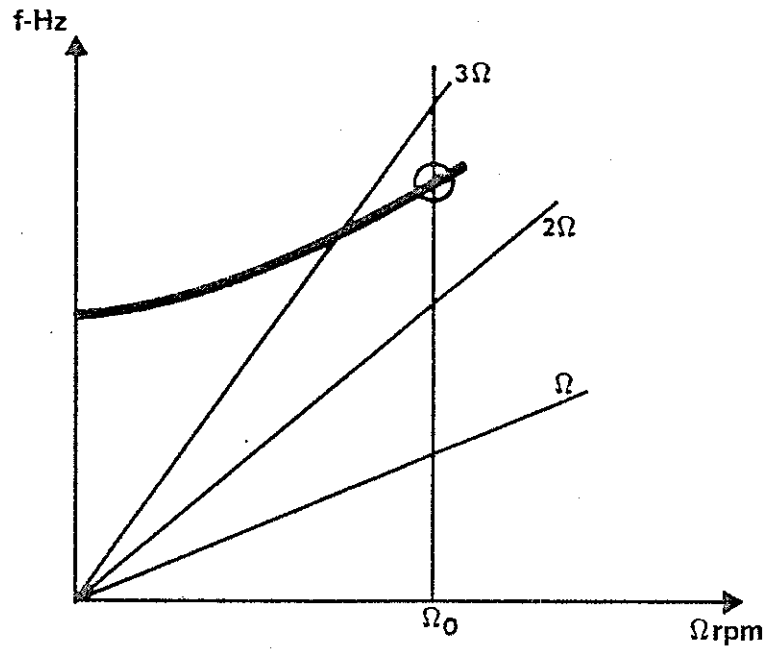


Fig. 5 — Rotor blade mode — Position of mode at nominal r.p.m.

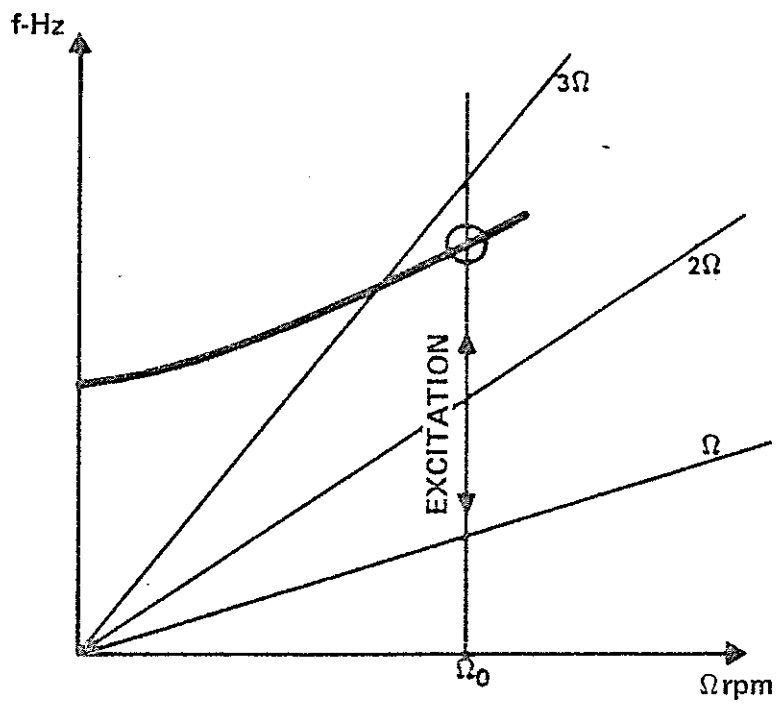


Fig. 6 — Rotor blade mode — Stabilized r.p.m. excitation principle